A novel African *Salmonella* Typhimurium ST313 sublineage with extensive drug-resistance and signatures associated with host adaptation

Authors:

Sandra Van Puyvelde[1,2,3*], Derek Pickard[2,4], Koen Vandelannoote[1], Eva Heinz[2,5], Barbara Barbé[6], Tessa de Block[1], Simon Clare[2], Eve L. Coomber[2], Katherine Harcourt[2], Sushmita Sridhar[2,4], Emily Lees[2,4], Nicole E. Wheeler[7], Elizabeth J. Klemm[2], Laura Kuijpers[6,8], Lisette Mbuyi Kalonji[9,10], Marie-France Phoba[9,10], Dadi Falay[11], Dauly Ngbonda[11], Octavie Lunguya[9,10], Jan Jacobs[6,8$], Gordon Dougan[2,4$], Stijn Deborggraeve[1$]

Affiliations

[1] Department of Biomedical Sciences, Institute of Tropical Medicine, Antwerp, Belgium

[2] Wellcome Sanger Institute, Wellcome Genome Campus, Hinxton, Cambridge, United Kingdom

[3] Laboratory of Medical Microbiology, Vaccine & Infectious Disease Institute, Universiteit Antwerpen, Antwerp, Belgium

[4] Department of Medicine, Addenbrookes Hospital, University of Cambridge, Cambridge CB2 0SP, United Kingdom

[5] Department of Vector Biology, Liverpool School of Tropical Medicine, Liverpool, UK

[6] Department of Clinical Sciences, Institute of Tropical Medicine, Antwerp, Belgium

[7] Centre for Genomic Pathogen Surveillance, Wellcome Sanger Institute, Wellcome Genome Campus, Hinxton, Cambridge, United Kingdom

[8] Department of Microbiology and Immunology, KU Leuven, Belgium

[9] Department of Microbiology, National Institute for Biomedical Research, Kinshasa, Democratic Republic of the Congo

[10] Department of Microbiology, University Hospital of Kinshasa, Democratic Republic of the Congo

[11] Department of Pediatrics, University Hospital of Kisangani, Kisangani, Democratic Republic of the Congo

[*] Corresponding author: svanpuyvelde@itg.be

[$] These authors contributed equally

Abstract

Bloodstream infections by *Salmonella enterica* serovar Typhimurium (*S.* Typhimurium) constitute a major health burden in sub-Saharan Africa (SSA). These invasive non-typhoidal (iNTS) infections are dominated by isolates of the antibiotic resistance-associated sequence type (ST) 313. Here, we report the emergence of a novel ST313 sublineage we name II.1 in the Democratic Republic of the Congo (DRC). Sublineage II.1 exhibits extensive drug resistance (XDR), involving a combination of multidrug resistance (MDR), extended spectrum betalactamase (ESBL) production and azithromycin (AZI) resistance. ST313 lineage II.I isolates harbour an IncHI2 plasmid we name pCST313 and some isolates also exhibit decreased ciprofloxacin susceptibility (DCS). Whole genome sequence analysis revealed ST313 II.I isolates have accumulated genetic signatures potentially associated with altered pathogenicity and host adaptation, in relation to changes observed in biofilm formation and metabolic capacity. Sublineage II.1 emerged at the beginning of the 21st century and is involved in on-going outbreaks. Our data provides evidence of further evolution within the ST313 clade of *S.* Typhimurium associated with iNTS in SSA.

Introduction

Salmonella enterica subspecies *enterica* serovar Typhimurium (*S.* Typhimurium) and other non-typhoidal *Salmonella* are common causes of gastrointestinal infections in people living in industrialized countries [1]. However, in sub-Saharan Africa (SSA), invasive non-typhoidal *Salmonella* (iNTS) bloodstream infections [2] are common totaling ~3.4 million cases annually, with *S.* Typhimurium being responsible for approximately two-thirds of these cases. The fatality rate in iNTS can be extremely high [3,4].

In SSA, iNTS patients often do not suffer from diarrhea but instead display symptoms of fever and septicemia [5]. There has been no proven zoonotic source of ST313 infections and human to human transmission has been postulated [6-8]. The disease disproportionately affects children under five years old and HIV positive adults [9].

Whereas the majority of *S.* Typhimurium associated with gastroenteritis in developed countries belong to sequence types (ST) 19 and 34, *S.* Typhimurium iNTS in SSA are predominantly of ST313 [10]. The population structure of *S.* Typhimurium ST313 is dominated by two clonal lineages, named I and II, that sequentially spread over SSA in the past 40 years [11]. The success of these ongoing pandemics has been attributed to resistance to antibiotics and the emergence of HIV [11,12]. The majority of iNTS *S.* Typhimurium isolated in the past 10 years have been of ST313 lineage II [13-15].

S. Typhimurium ST313 isolates are predominantly multidrug resistant (MDR), implying co-resistance to the three former first line antibiotics ampicillin, trimethoprim/sulfamethoxazole and chloramphenicol [16,17]. Two recent genomics-based studies reported the acquisition of extended-spectrum β-lactamases (ESBLs), conferring resistance to the third generation cephalosporin ceftriaxone, among *S.* Typhimurium ST313 lineage II isolates from Malawi and Kenya [13,14]. Ceftriaxone is a

recommended antibiotic to treat complicated iNTS, while the fluoroquinolone ciprofloxacin is recommended for uncomplicated iNTS [18].

The genomes of *S.* Typhimurium ST313 show evidence of specialization towards a narrow host range by pseudogenization in a pattern that resembles that found in the host restricted typhoidal *Salmonella S.* Typhi [5,19,20]. The genotypic differences between ST313 and ST19 isolates have been confirmed as phenotypes associated with host virulence and other traits, such as biofilm formation which has been postulated to influence both survival in the environment and macrophages [11,21-25].

Here, we report the emergence of a novel extensively drug resistant (XDR) ST313 sublineage, we name II.1, which is currently causing bloodstream infections in the Democratic Republic of the Congo (DRC) and represents > 10 % of all *S.* Typhimurium isolated in the Kongo Central Province [17]. This sublineage is associated with a combination of MDR, ESBL production and resistance to azithromycin (AZI). Additionally, whole genome sequencing of multiple genomes identified signatures associated with pathogenicity, metabolism and potentially host adaptation.

Results

1. An XDR *S.* Typhimurium ST313 sublineage II.1 is emerging in the DRC

Invasive *S.* Typhimurium have been isolated in different hospital sites across DRC during ongoing microbial surveillance of bacterial bloodstream infections [17,26,27]. As third generation cephalosporins and AZI have been used in treatment we have monitored susceptibility using both phenotypic and genetic approaches. Consequently, to investigate the emerging phenotype of ESBL production and AZI resistance, a selection of 81 *S.* Typhimurium isolates from the region were subjected to whole genome sequence analysis. Their year and place of origin, the age of the

patient and their phenotypic antimicrobial susceptibility are listed in Supplemental Table 1. Of this panel, 54 *S.* Typhimurium isolates exhibited AZI resistance and were ESBL positive; all except three were also MDR and are thus classifiable as XDR. The isolates were collected from 2008 to 2016 in western (Kisantu, Kongo Central Province n=50; Kinshasa n=2) and northeastern DRC (Kisangani, Tshopo Province: n=2) (Fig. 1). Minimum inhibitory concentration (MIC) values for AZI resistance were between 32 and >256 mg/l. Two of these isolates, 5390_4 (Kisangani, 2016) and 2735 (Kinshasa, 2008), showed decreased susceptibility to the fluoroquinolone ciprofloxacin (decreased ciprofloxacine susceptibility (DCS), MIC values of 0.38 and 0.19 mg/l against ciprofloxacin respectively). These isolates also exhibited resistance to the quinolone pefloxacin, and susceptibility (5390_4) or resistance (2735) to the quinolone nalidixic acid. The other 27 *S.* Typhimurium isolates form a representative local context, originating from bloodstream infections in the same surveillance sites in DRC (see Supplementary Note). They were isolated between 2007 and 2016, and show no ESBL production nor resistance to AZI. The majority of these isolates (22 out of 27) were MDR. One isolate, 16755_3 (Kisantu, 2016), exhibited DCS with a MIC value of 0.19 mg/l.

Multilocus sequence typing (MLST) confirmed that all belong to ST313. An optimal context for the genomic analysis was obtained by including 153 African [11,14,15,28,29] and 42 non-African [11] *S.* Typhimurium genomes in the overall analysis. The complete list of 276 analyzed *S.* Typhimurium genomes with the year, place and source of isolation is presented in Supplemental Table 2.

This analysis revealed a novel sublineage II.1 in DRC defined by the most recent common ancestor of the monophyletic sublineage of 51 XDR isolates (Fig. 2.A). One isolate, 5390_4, originating from Kisangani (2016) while being MDR, ESBL

producing, AZI resistant and showing DCS, falls outside sublineage II.1, but is part of the clonal lineage II. All 27 control isolates also fell into lineage II, with two older isolates from Kisantu (2009) being most closely related to sublineage II.1 (1577 and 1582).

The *S.* Typhimurium ST313 lineage I and II in our study accumulated respectively 225 and 216 conserved single nucleotide polymorphisms (SNPs) in their core genomes compared to their most recent common ancestor (Supplemental Fig. 1), which is comparable to previous observations [20]. In comparison to the lineage II clade, sublineage II.1 isolates, except 2735, accumulated an additional 38 conserved core SNPs, and show a clonal structure with little substructure (Fig. 2b). Of note, the two isolates showing an AZI MIC value > 256 mg/l form a monophyletic clade within sublineage II.1 (17399_3 and 17568_3). No SNPs were acquired in known genes involved in macrolide resistance [30], but both isolates have a G118V amino acid substitution in the ABC-transporter protein BtuC. This SNP, in addition to the presence of *mphA*, might be involved in the observed increased AZI resistance [31]. Cephalosporin resistant ST313 lineage II infections were previously reported from Kenya and Malawi [13-15]. The XDR isolates we describe here form a novel ST313 sublineage II.1.

The putitive origin of the ST313 lineage II was previously predicted to be the DRC [11]. Consequently, we applied a temporal reconstruction using BEAST2 to the *S.* Typhimurium ST313 lineage II and II.1 isolates. This limited analysis indicates that sublineage II.1 may have emerged in the DRC around 2004 (95% highest probability density (HPD) interval: 2000-2007) (Fig. 3).

2. **Lineage II.1 harbours a novel IncHI2 resistance plasmid, pCST313**

A comprehensive resistome, composed of all catalogued genetic determinants for AMR, was bioinformatically extracted from the sequencing data (Supplemental Table 2). This analysis indicated that the MDR phenotype observed in *S.* Typhimurium ST313 lineage II and sublineage II.1 isolates is associated with genes predicted to confer resistance to chloramphenicol (*catA*), ampicillin (*blaTEM1*) and trimethoprim (*dfrA*). While lineage II is linked to the presence of *dfrA1*, this allele is replaced by *dfrA14* in sublineage II.1. XDR sublineage II.1 isolates harbour *blaSHV-2A* and *mphA* genes, respectively potentially associsated with resistance to cephalosporins and azithromycin. Identical *blaSHV-2A* and *mphA* genes are present in the ESBL positive, AZI resistant lineage II isolate from Kisangani (5390_4). One sublineage II.1 isolate, 2735, shows DCS (MIC value ciprofloxacin = 0.19 g/l) in addition to AZI resistance and ESBL production and harbours a mutation in *gyrA* (D87N) associated with DCS. DCS combined with ESBL positivity and AZI resistance was also observed in the lineage II isolate 5390_4 (Kisangani, 2016, MIC value ciprofloxacin = 0.38 g/l), which has acquired a *qnrS* gene. The lineage II isolate 16755_3 (Kisantu, 2016, MIC value ciprofloxacin = 0.19 g/l), showing DCS but no ESBL activity nor AZI resistance and harbours a S83Y mutation in *gyrA.*

All sublineage II.1 isolates as well as the lineage II 5390_4 isolate (ESBL + AZI) from Kisangani harbour a IncHI2 plasmid. IncHI2 plasmids have been reported previously in other *S.* Typhimurium ST313 isolates from Kenya (pKST313) and Malawi (pSTm-A54650) [13,14]. We have named the novel “Congolese” IncHI2 plasmid pCST313, in analogy to the Kenyan pKST313 IncHI2 plasmid [13]. The full pCST313 plasmid sequence associated with sublineage II.1 was determined using PacBio sequencing of isolate 10433_3 (Kisantu, 2014). pCST313 is 274,695 nucleotides (Fig. 4) and is highly conserved among all sublineage II.1 isolates, differing by ~5 single

SNPs between isolates. The known AMR determinants of ST313 sublineage II.1 are located on pCST313, as well as genes associated with heavy metal resistance against silver and copper. pCST313 encodes a potentially active TraB conjugation protein and conjugation operon [32].

pCST313 exhibits significant similarity to R478 (99% identity over 86% coverage of pCST313), a self-transferable IncHI2 plasmid isolated from *Serratia marcescens* in 1969 in the USA [33]. Pairwise sequence comparisons of pCST313 with the other IncHI2 plasmids (1) pKST313 from Kenya, (2) pSTm-A54650 from Malawi, a (3) draft assembly from the IncHI2 plasmid of 5390_4 from Kisangani and R478 revealed significant similarity between the plasmid backbones (Fig. 4 and Supplemental Table 3). The less conserved regions of pCST313 include antimicrobial resistance genes, flanked by transposon-associated regions (Fig. 4).

3. The gemomes of *S.* Typhimurium ST313 lineage II.1 exhibit genetic signatures of altered pathogenicity and host adaptation

ST313 sublineage II.1 harbours multiple chromosomal sequence differences in comparison to ST313 lineage II isolates (Figure 5). A deletion of 1076 nt was observed in the chromosome of ST313 sublineage II.1, resulting in loss of *fljB.* The *fljB* gene codes for the phase 2 flagellin protein which polymerizes to form the bacterial flagella (Supplemental Fig. 4). Loss of *fljB* (FljB) was confirmed at the DNA and protein level (Supplemental Fig. 5). Consequently, in contrast to their biphasic ancestors, sublineage II.1 isolates are monophasic as they only harbour the phase 1 flagellin gene, *fliC.*

We annotated the SNPs that are acquired in ST313 sublineage II.1 relative to lineage II (Supplemental Table 4). Of these SNPs, 19 are present in coding regions and cause

predicted non-synomynous mutations in the protein sequence (Supplemental Table 4). Seven of these 19 SNPs are located in conserved Pfam protein domains resulting in deviant bitscores. Consequently, we prioritized these SNPs as the most likely to cause functional defects. The affected genes are geranyltranstransferase *ispA*, methyl-accepting chemotaxis protein *trg_1*, precorrin-3B C17-methyltransferase *cbiH*, propanediol dehydratase reactivation protein, outer membrane assembly protein *asmA*, putative multidrug export ATP-binding/permease protein SAV1866 and putative diguanylate cyclase *yhjK*. These genes have been linked to host-adaptation (*cbiH*) [19], virulence associated processes (*asmA*) [34] and chemotaxis during infection (*trg_1*) [35]. Of note, these molecular processes are also linked to pseudogene acumulation in the phylogeny from *S.* Typhimurium ST19 to ST313 lineage II [20].

As our interpretations are likely biased by the available literature, we applied a data mining approach to obtain a more objective evaluation of the association between the acquired SNPs in sublineage II.1 and invasiveness. Hereto, the *Salmonella* invasiveness index of each strain was calculated, which is based on the genomic signatures for *S. enterica* associated with adaptation to an invasive lifestyle [36]. We observe an increase in invasiveness index from non-ST313 and ST313 lineage I strains to lineage II, and a significant further increase of the invasiveness index from lineage II to lineage II.1 (Fig. 6a, Supplemental Fig. 5).

In addition to the observed genomic differences, *S.* Typhimurium ST313 sublineage II.1 isolates exhibited measurably different phenotypes compared to *S.* Typhimurium ST313 lineage II. A red dry and rough (RDAR) biofilm assay was performed that uses agar plates with stains that reveal extracellular matrix production in colonies. In this assay, *S.* Typhimurium ST313 lineage II isolates lost the rough morphotype compared to ST19, changing from a red, dry and rough (rdar) to a brown and smooth (bas)

phenotype. This phenotype was shown previously to be due to defective production of cellulose, one of the two major extracellular components of *Salmonella* biofilms [21,23]. Interestingly, *S.* Typhimurium ST313 lineage II.1 shows a further defect in biofilm formation. Sublineage II.1 isolates have a smooth and white (saw) colony morphotype in this assay, whereas sublineage II isolates have a brown and smooth (bas) morphotype (Fig. 6b). This phenotypic defect is consistent across all isolates from sublineage II.1 and resembles the *S.* Typhi morphotype. The exception was isolate 2735 (Kinshasa, 2008), the phylogenetically oldest representative of sublineage II.1 (Supplemental Fig. 6) [22]. Among the SNPs that were acquired in sublineage II.1 compared to lineage II, none were located in or near genes responsible for the production of curli, which is another major biofilm compound. Mutagenesis experiments showed that the introduction of a null mutation into the *asmA* gene of *S.* Typhimurium ST313 lineage II D23580 partly recreated the sublineage II.1 biofilm phenotype (Fig. 6b), suggesting that the non-synomynous SNP in *asmA* might contribute to the biofilm defect. *asmA* encodes an outer membrane protein that was previously described to be involved in the invasion of epithelial cells [34]. Targeted mutations in *wzxC*, *yhjJ* and *yhjK* in D23580 had no obvious effect on the biofilm phenotype (Supplemental Fig. 7).

While *Salmonella* causing gastrointestinal infections typically have a relatively large metabolic capacity, strains causing invasive infections generally have a more limited capacity [37]. We used Biolog Phenotype Microarrays to assess growth on 192 different metabolic compounds between two representative isolates of both lineage II and lineage II.1. Lineage II.1 isolates showed significant lower metabolic capacity for carbon compounds compared to lineage II isolates (Supplemental Table 5). The effect was most pronounced for D-galactonic acid γ-lacton (Supplemental Fig. 8).

We also assessed the phenotypic behaviour of five representative sublineage II.1 isolates in *in vitro* and *in vivo* models. Human macrophage cell killing assays, intravenous and oral mice infections did not show significant differences between the lineages, although two sublineage II.1 isolates showed an overall lower infection of THP macrophages and cell counts in mice deep tissue after intravenous infections (Supplemental Fig. 9, 10 and 11).

Discussion

Here, we report the emergence of a novel *S.* Typhimurium ST313 sublineage II.1 from the DRC with unprecedented levels of AMR. The World Health Organisation (WHO) has listed *Salmonella* spp. as one of the pathogens for which new antibiotics are urgently needed [38]. In addition to the MDR phenotype of lineage II [11], sublineage II.1 is associated with ESBL activity, AZI resistance and occasional DCS, thereby giving rise to the first lineage of XDR iNTS. As there is no XDR definition for iNTS yet, we extrapolate the definition from XDR *Salmonella enterica* subspecies *enterica* serovar Typhi (*S.* Typhi), recently defined as resistance to five antibiotics (observed as MDR combined with resistance against fluoroquinolones and ESBL activity), thereby using the same nomenclature as for other bacterial pathogens [39,40]. The XDR iNTS isolates from this study show MDR in combination with resistance to the two alternative treatment options ceftriaxone and AZI.

Sublineage II.1 was identified in three independent surveillance sites in the DRC, suggesting this sublineage is relatively widespread in the region, although further surveillance is required to confirm the burden [17,41-43].

All except three of the *S.* Typhimurium ST313 lineage II.I isolates described here fall into the XDR category defined for *S.* Typhi [39,40]. Within the DRC setting, the only

available antibiotic for treatment of XDR iNTS infections are fluoroquinolones. Importantly, DCS iNTS is present in DRC, with one pan-resistant (XDR + DCS) isolate identified in this study. The use of fluoroquinolones might cause serious side effects involving muscles, tendons, bones and the nervous system recently urging the European Medicines Agency Pharmacovigilance Risk Assessment Committee (PRAC) to recommend restricting the use [44]. As a consequence, the emergence of this XDR iNTS sublineage II.1 increases the urgency for advancements in other strategies to combat the disease, such as vaccination.

Antibiotic use might have provided the selection pressure driving the emergence of this sublineage. Within SSA, the antibiotic AZI has been used in mass drug administrations for the elimination of Trachoma, and has also recently been tested to reduce childhood mortality [45,46]. In the DRC, it is not clear which antibiotics are in routine use, as only 30% of patients have access to the regular healthcare system, and 40% rely on self-medication [47]. MDR in ST313 sublineage II.1 is linked here with the IncHI2 plasmid pCST313. Intriguingly, previous reports have associated iNTS *S.* Typhimurium in SSA with IncHI2 plasmids [13,14,48].

The acquisition of antibiotic resistance and the accumulation of genomic signatures associated with host adaptation by sublineage II.1 suggest further specialization to a human niche [49,5012,20,21]. Sublineage II.1 are monophasic, a phenotype similar to typhoidal *Salmonella* [50]. A large recombination event took place at the *fljB* locus, resulting in loss of phase II flagellin production, while the phase I flagellin gene *fliC* remained intact. Bacterial flagellin plays an important role in the host innate immune response and is a stimulator of innate immunity through Tlr5 [51,52]. Strikingly, a pandemic of monophasic *S.* Typhimurium ST34 causing gastro-intestinal infections has recently been identified, with some strains of this pandemic causing bloodstream

infections in Vietnam [53,54]. Sublineage II.1 have a reduced capacity to form multicellular communities compared to lineage II [21], again with similarity to *S.* Typhi [22]. Bacterial biofilms are important for both resistance to environmental stresses and survival outside the host. *S.* Typhimurium ST313 sublineage II.1 isolates also show a lower capacity for the metabolism of carbon sources, in line with the findings that *S.* Typhimurium ST313 has a reduced metabolic capacity compared to *S.* Typhimurium ST19 [20].

Survival in macrophages was experimentally assessed, given the observed mutations in sublineage II.1, such as loss of *fljB*, which can affect macrophage survival [23]. However, we did not find significant differences between lineage II and sublineage II.1 in macrophage infection assays. Likewise, II.1 isolates did not show a reproducible increased colonization of deeper tissue during intravenous or oral mouse infections. Although our genomic, biofilm and metabolic data show signatures for increased human adaption of lineage II, *S.* Typhimurium ST313 lineage II.I isolates are thus not host restricted.

In conclusion, in this study we identified an on-going outbreak of a novel sublineage II.1 emerging from the current African *S.* Typhimurium ST313 pandemic. Sublineage II.1 is associated with XDR driven by an IncHI2 plasmid named pCST313, harbouring resistance to AZI and ESBL production. In addition, sublineage II.1 also shows evolutionary signatures associated with host adaptation. Extended bloodstream surveillance in the endemic regions of *S.* Typhimurium ST313 will be crucial to further track the spread of XDR ST313 sublineage II.1 and to timely detect the emergence of new sublineages with novel antibiotic resistance profiles

Methods

1. Selection of bacterial isolates from bloodstream surveillance

The DRC isolates originated from blood cultures sampled at the referral hospital of Saint Luc in Kisantu (Kongo Central province), the University Hospital of Kinshasa, the referral Hospital St. Joseph and Monkole Hospital from Kinshasa (Kinshasa province), the referral hospital of Bwamanda (Tshopo province), the referral hospital of Kabondo and the university hospital of Kisangani (CUKIS) and associated health centers (Sud-Ubangi province) in the DRC [17,27,43]. These hospitals have participated in the microbiological surveillance network since 2007 coordinated by the National Institute of Biomedical Research (INRB) in Kinshasa, DRC, in collaboration with the Institute of Tropical Medicine (ITM) in Antwerp, Belgium. Blood cultures were sampled in patients suspected of bloodstream infections according to standard indications and methods as described elsewhere [17].

All available XDR *S.* Typhimurium available to this study were included (n=54). A sample of 27 representative non-XDR *S.* Typhimurium isolates were selected as controls for this analysis. Most health facilities across the country lack capacity for diagnosing bacterial bloodstream infections and we have therefore no information about bloodstream infections elsewhere in DRC except as part of outbreak research [41,42]. The surveillance sites included in this study were not consistently active because of stock ruptures, staff movements, funding and insecurity. All isolates were stored in tubes of Trypticase Soya Agar (Oxoid, Basingstoke, UK) and shipped to ITM for confirmation and further identification.

At ITM, isolates biochemically confirmed as *Salmonella* spp. were serotyped using commercial antisera (Sifin, Berlin, Germany) according to the Kauffmann-White scheme [55]. A representative selection of the isolates (10%) was sent to the National Reference Centre in Belgium for confirmation of serotype. Antibiotic susceptibility

353 testing of all isolates was done by disk diffusion (Neo Sensitabs, Rosco, Taastrup,
354 Denmark) according to the National Committee for Clinical Laboratory Standards
355 (CLSI) guidelines; for ciprofloxacin and AZI, minimal inhibitory concentration
356 (MIC-values) were determined with the E-test macromethod (bioMérieux).
357 Interpretation of results was performed according to the most recent CLSI guideline
358 [56]. Isolates with intermediate susceptibility were considered resistant. MDR was
359 defined as co-resistance to all three first-line antibiotics ampicillin, chloramphenicol
360 and trimethoprim-sulfamethoxazole [18]. Extended-spectrum β-lactamase (ESBL)
361 production was assessed by double disk method according to CLSI guidelines [56]. For
362 ciprofloxacin, the susceptibility breakpoint of $\leq$ 0.064 mg/L was used; the term
363 "decreased ciprofloxacin susceptibility" was used to indicate MIC values > 0.064
364 mg/L and < 1 mg/L, and "ciprofloxacin resistance" was reserved for MIC values $\geq$ 1
365 mg/L [56]. For AZI, isolates were considered resistant at MIC values $\geq$ 16 mg/L [56].
366 Ethical approval for the Microbiological Surveillance was granted by the Institutional
367 Review Board at the ITM in Antwerp, by the Ethics Committees of the Antwerp
368 University (Belgium) and the School of Public Health (Kinshasa, DRC).
369

370 **2. Illumina and Pacbio whole genome sequencing**

371 DNA from all 81 strains was purified using the Gentra PureGene Yeast/Bact Kit
372 (Qiagen, Hilden, Germany), following the manufacturer's guidelines and DNA was
373 sequenced on an Illumina HiSeq platform (Illumina, San Diego, USA). Illumina
374 adapter content was removed from the reads using Trimmomatic v.0.33 [57]. Public
375 available Illumina sequencing data from 153 *Salmonella* Typhimurium strains
376 originating from DRC, Mali, Nigeria, Uganda, Kenya, Malawi and Mozambique and
377 a selection of 42 non-African genomes were included in the further genomics analysis

[11,13-15,29]. This is a convenience sample including all publicly available African iNTS genomes. Strains are summarized in Supplemental Table 2.

A high-quality reference genome sequence of sublineage II.1 isolate 10433_3 was constructed using the PacBio RS II platform (PacBio, Menlo Park, CA, USA). The PacBio Template Prep Kit (PacBio, Menlo Park, CA, USA) and BluePippin™ Size Selection System protocol were used to prepare size-selected libraries (20kb) from 5 μg of sheared and concentrated DNA. Sequencing was performed using the magnetic bead collection protocol, a 20,000 bp insert size, stage start, and 180-minute movies. Sequence reads were assembled using HGAP v3 28 of the SMRT analysis software v2.3.0 (Pacbio, Menlo Park, CA, USA). The fold coverage to target when picking the minimum fragment length for assembly was set to 30 and the approximate genome size was set to 3Mbp. The assembly was circularized using Circlator v1.1.3 [58]. Finally, the circularized assembly was polished using the PacBio RS_Resequencing protocol and Quiver v1 of the SMRT analysis software v2.3.0 [59]. Automated annotation was performed using PROKKA v1.11 [60] and genus specific databases from RefSeq [61]. The final assembled bacterial chromosome consisted of 4,877,289 bp, and two plasmid sequences of 274,695 bp and 94,649 bp.

3. Read mapping, variant detection and phylogenetic analysis

Illumina HiSeq reads were mapped to the *Salmonella* Typhimurium reference genomes of ST313 lineage II (D23580, FN424405.1, [12]) and ST313 sublineage II.1 (10433_3, this study) using SMALT v0.7.4 to produce a BAM file.

SMALT was used to index the reference using a kmer size of 20 and a step size of 13 and the reads were aligned using default parameters but with the maximum insert size set as 3 times the mean fragment size of the sequencing library. PCR duplicate reads

were identified using Picard v1.92 (Broad Institute, Cambridge, MA, USA) and flagged as duplicates in the BAM file.

Variation detection was performed using samtools mpileup v0.1.19 with parameters "-d 1000 -DSugBf" and bcftools v0.1.19 [62] to produce a BCF file of all variant sites. The option to call genotypes at variant sites was passed to the bcftools call. All bases were filtered to remove those with uncertainty in the base call. The bcftools variant quality score was required to be greater than 50 (quality < 50) and mapping quality greater than 30 (map_quality < 30). If not all reads gave the same base call, the allele frequency, as calculated by bcftools, was required to be either 0 for bases called the same as the reference, or 1 for bases called as a SNP (af1 < 0.95). The majority base call was required to be present in at least 75% of reads mapping at the base, (ratio < 0.75), and the minimum mapping depth required was 4 reads, at least two of which had to map to each strand (depth < 4, depth_strand < 2). Finally, strand_bias was required to be less than 0.001, map_bias less than 0.001 and tail_bias less than 0.001. If any of these filters were not met, the base was called as uncertain.

A pseudo-genome was constructed by substituting the base call at each site (variant and non-variant) in the BCF file into the reference genome and any site called as uncertain was substituted with an N. Insertions with respect to the reference genome were ignored and deletions with respect to the reference genome were filled with N's in the pseudo-genome to keep it aligned and the same length as the reference genome used for read mapping.

Recombinant regions in the chromosome such as prophage regions and the *fljB* ORF in the chromosome were removed from the alignment and checked using Gubbins v1.4.10 [63]. SNP sites were extracted from the alignment using snp-sites [64] and used to construct a maximum likelihood phylogeny. RAxML v8.2.8 [65] with substitution

model GTRCAT. Support for nodes on the trees was assessed using 1000 bootstrap replicates. A comprehensive tree, with reads mapped to ST313 lineage II (D23580, FN424405.1, [12]) was rooted on *S.* Paratyphi A270 (ERR326600). Based on this tree, lineage II and sublineage II.1 isolates were identified and a high-resolution lineage II tree was constructed based on mapping to ST313 sublineage II.1 (10433_3, this study) and rooted to *S.* Typhimurium ST313 strain DT2. Trees were visualized using Figtree v1.4.2 and iTOL [66]. The comprehensive phylogenetic tree with spatiotemporal metadata, based on mapping against D23580 and rooted on *S.* Paratyphi A270 is made publicly available on MicroReact [67] (https://microreact.org/project/9f_SsS82d, Supplemental Fig. 2).

4. Bayesian phylogenetic & phylogeographic analysis

We used BEAST2 v2.4.8 [68] to date evolutionary events, determine the substitution rate and produce a time-tree of African *S.* Typhimurium with tip-dates defined as the year of isolation (Supplemental Table 2). BEAUti xml's were manually modified to specify the number of invariant sites in the genome. We employed a general time reversible (GTR) substitution model with gamma distributed rate heterogeneity. In addition, an uncorrelated log-normal relaxed molecular clock [69] was used to model the variation of evolutionary (substitution) rates across branches. The extended Bayesian skyline plot (EBSP) demographic method [70] was selected as this model does not depend on a prespecified parametric model of demographic history and the method has been proven to indicate the most appropriate demographic model for any given dataset. Earlier BEAST analyses on a related dataset identified the molecular clock model and tree prior used here to have the highest support by using Bayes factor (ratio of the marginal likelihoods of two competing models) based model selection [11].

All parameters were estimated jointly in a BEAST2 analysis using a total of 10 independent chains of 500 million generations, with samples taken every 50,000 MCMC generations. Log files were inspected in Tracer v1.6 for convergence, proper mixing, and to assess whether the chain length produced an effective sample size (ESS) for all parameters larger than 300, indicating sufficient sampling. LogCombiner v2.5.0 was used to combine log and tree files of the independent BEAST2 runs, after having removed a 30% burn-in from each run. Thus, parameter medians and 95% highest posterior density (HPD) intervals were estimated from 70,000 sampled MCMC generations. The entire analysis was replicated on five random subsets of 100 taxa of the complete isolate panel to test if our results were affected by sampling bias. To ensure prior parameters were not over-constraining the calculations, the entire analysis was also run while sampling only from the prior, and the resulting parameter distributions were compared in Tracer. Finally, TreeAnnotator v2.5.2 was used to summarize the posterior sample of time-trees in order to produce a maximum clade credibility tree with the posterior estimates of node heights visualized on it.

5. Genomic rearrangements and SNP analysis

Large genomic rearrangements were identified by analysis of the aligned reference genome sequences using the Artemis Comparison Tool (ACT).

A VCF file containing all SNP sites was extracted using snp-sites [64] from all strains included in this study. Conserved SNPs between lineage II and lineage II.1 strains were extracted using custom calculations in R v.3.3.3, thereby comparing SNPs with the D23580 reference sequence and annotation (FN424405.1). SNPs that were conserved in 51 of the 53 sublineage II.1 strains, and not present in lineage II strains were subjected to a functional analysis. These SNPs were functionally studied by

comparison with the D23580 annotation [12]. Ortholog loci in *S.* Typhimurium LT2 (NC_003197.2) were identified using BLASTN 2.6.0+.

For SNPs present in coding regions, the effect of the SNP on the respective amino acid sequence was assessed. For non-synonymous SNPs, the PAM1 value and delta bitscore value was included. The higher the PAM1 value, the more frequent specific amino acid substitutions are observed. Delta bitscores were calculated by subtracting the bitscore for a given HMM domain in lineage II from the bitscore of the orthologous domain lineage II.1 strains [71].

To calculate the invasiveness index per strain, sequence reads of each sample were mapped against the *S.* Typhimurium SL1344 reference genome (FQ312003.1) using BWA mem v0.7.12 [72] to produce a BAM file. BWA was used to index the reference and the reads were aligned using default parameters but with the maximum insert size set as 3 times the mean fragment size of the sequencing library. Picard (http://broadinstitute.github.io/picard) was used to identify and flag optical duplicates generated during library preparation. SNPs and indels were called using samtools v1.2 mpileup [73], and were filtered to exclude those variants with coverage <10 or quality <30. SNP calls were used to produce variant coding sequences. Protein sequences were then screened using phmmer to identify the closest homologs to the 196 predictive genes used by the invasiveness index model. These genes were then scored against profile hidden Markov models (HMMs) for these protein families from the eggNOG database to test for uncharacteristic patterns of sequence variation. Bitscores produced in the comparison of each protein sequence to its respective protein family HMM were then used as input to the model. The groups were compared using a Mann Whitney U test.

6. Sequence typing, resistance gene analysis and plasmid analysis

Resistance genes were determined from the raw Illumina sequencing data using ariba v 2.11.1 [74] with CARD database version 1.1.8 [75]. SNPs explaining a DCS phenotype was checked individually for strains showing DCS. The *gyrA*, *gyrB*, *parC*, *parE*, *acrB* sequences of reference sequence from *S.* Typhimurium LT2 (NC_003197.2) were compared to assemblies of the DCS strains using BLASTN 2.6.0+. The presence of plasmid replicons was determined from raw Illumina reads using SRST2 [76] with the complementary P18 plasmid replicon database.

The PacBio reference sequence of plasmid pCST313 (*S.* Typhimurium DRC, this study) was searched for similar nucleotide sequences publicly available using using NCBI Blast with the Nucleotide collection (nt), update 2017/07/13. Pairwise comparisons were done using BRIG [77]. pCST313 was compared with plasmids R478 (*Serratia marcescens* USA, BX664015), pKST313 (*S.* Typhimurium, LN794248) and pSTm-A54650 (*S.* Typhimurium, LK056646). A *de novo* assembly was performed based on Illumina sequences of isolate 5390_4 (This study) [78] and the assembly of the plasmid sequence was used for pairwise comparative analysis. Hereto, the contigs of the assembly were reordered using Mauve version 2015_02_25 [79] and the 12 contigs homologous to pCST313 were retained for further analysis.

7. Flagella expression

Presence of *fljB* (FljB) and *fliC* (FliC) were confirmed at the DNA and protein level for a *S.* Typhimurium reference lineage II (isolate 9412_3) and sublineage II.1 (10433_3) strain. DNA was extracted from both strains using Gentra Puregene Yeast/Bact. Kit (Qiagen, U.S.A) and PCR-amplified using *fljB* (forward GCT CCT GTC GCT TCA TCG TA, reverse ACG GTA CAG TAA CCC TTG CG) and *fliC*

(forward AAC AGA TGC TGT GCC GGT AA, reverse CTC GGC TAC TGG TCT TGG TG) specific primers.

For protein samples, overnight cultures were centrifuged at 1500 g and pellets were suspended in 300µl phosphate-buffered saline (PBS, pH 7.4). The suspension was homogenized using FastPrep-24 (MP Biomedicals, Santa Ana, California, USA) and centrifuged at 15000 rpm. 10 µl of the supernatant was diluted 1:1 with sample buffer (Laemmle, Sigma-Aldrich, St. Louis, Missouri, US) before loading on SDS-page gel (12%). After running (45 min 100V) the gel was colored with Coomassie blue.

8. Biofilm assays

Strains were grown in 10 ml low salt LB Broth overnight, diluted 1:100 in phosphate-buffered saline (PBS) and 5µl was spotted onto Red-Dry-Rough (RDAR) Phenotype plates (1.5% Agar, 1% Tryptone, 0.5% Yeast Extract, 20 µg/ml Coomassie Brilliant Blue, 40 µg/ml Congo Red in water) [80]. The plates were incubated at 27°C without inversion for 84 hours, phenotype analysed and photographed. Colonies were quantitatively analysed using the IRIS software [81].

9. Biolog assays

Four *S.* Typhimurium ST313 lineage II (12299_3, 9266_3, 9412_3 and D23580) and four *S.* Typhimurium sublineage ST313 sublineage II.1 (10393_3, 10433_3,12306_3 and 8866_3) isolates were analysed on the OmniLog phenotype MicroArray (PM) platform, in three independent biological replicates each. Overnight cultures cells were transferred with a sterile swab to 15 ml IF-0 (12.5 ml IF-0 with 2.5 ml H_2O) and stirred to obtain a uniform suspension. Turbidity of the suspension was adjusted to 42% transmittance T by using the Biolog Turbidimeter. Plates PM 1 and PM 2 were

inoculated with 100µl per well of the cell suspension mix diluted 1:5 in IF-0 containing 1.2% dye mix A. All plates were covered by anaerobic sealing foil (Roche) and incubated in the Omnilog phenotype MicroArray system for 48h at 37°C. Statistical calculations and visualization were done in R [82] by using the opm package [83]. The curve parameters were estimated using spline fitting. The mean of the area under the curve (AUC) was compared between sublineage II.1 versus lineage II strains using a linear model based on a 'Tukey'-type contrast using the opm_mcp function from the multcomp package [84].

10. Mutant construction

Mutant strains *S.* Typhimurium D23580 Δ*asmA*, *S.* Typhimurium D23580 Δ*yhjJ*, *S.* Typhimurium D23580 Δ*yhjK* and *S.* Typhimurium D23580 Δ*wxzC* were constructed. Hereto, the Kanamycin resistance gene (*kan*) was PCR-amplified from pKD4 using Q5 HotStart DNA Polymerase (New England Biolabs, Massachusetts, U.S.A.) and gene specific oligos (Integrated DNA Technologies, Illinois, U.S.A.) for *asmA* (TGAGACGATTTCTGACGACGCTGATGATTCTCCTGGTCGTGCTGGTGGCCTGTGTAGGCTGGAGCTGCTTCG, GGCCTGCTGCACCAGTTGCTGGAAATTCATTCCTTCAAGGCGCGTATTGCCATATGAATATCCTCCTTAG), *wxzc* (GGCGCTAAATGGTCGGCTATCGCCACGATAGTGATTATCGGTCTGGGGTTTGTGTAGGCTGGAGCTGCTTCG, CCCCGCCAGATGGCCGCCAATGAGAATTGCCGGGATAAACAGAAACGTTTCATATGAATATCCTCCTTAG), *yhjJ* (GATCGTATTGAAGTTCGTCTCCAGGTTAATACCGGTTCGCTCACCGAAAGTATGTGTAGGCTGGAGCTGCTTCG, GATAGCTGCTGACGTAAATTCTGATTGAGCATATCAACGGTCAGGCTGTTGACATATGAATATCCTCCTTAG) and *yhjK* (CTGGTACAGCAGAACCGCTACAACACGGCTACGCAACTGGAAAGCATCGCTGTGTAGGCTGGAGCTGCTTCG, CAGGGTGCATGAGCTGTAACGCGGAAAGATTGACGGAGAGCGGCAATGTCCATATGAATATCCTCCTTAG). DNA was prepared by gel extraction (Qiagen, Hilden, Germany) and ethanol precipitation.

The pSIM18 vector carrying the lambda RED recombinase system [85] was electroporated into *S.* Typhimurium D23580 using 10.5 ng DNA at 2.5 kV, 200 ohms, 25 µF (Bio-Rad MicroPulser, California, U.S.A.). The subsequent *S.* Typhimurium D23580::pSIM18 was used to create the mutant strains.

S. Typhimurium D23580::pSIM18 was grown overnight and then diluted 1 in 100 the next day in low salt LB plus 100 µg/ml Hygromycin B (Thermo Fisher, Massachusetts, U.S.A.) and incubated for 3 hrs, shaking at 30 ^{o}C to an OD^{590} of 0.4. The culture was spun for 10 min at 2500 x g and washed twice in ice cold 10% glycerol. The cell pellet was finally resuspended in 140 µl of 10% glycerol and electroporated with DNA (Table 1) in a precooled 2mm electroporation cuvette under conditions specified previously. Cells were then incubated in 500 µl of pre-warmed SOC outgrowth medium (New England Biolabs, Massachusetts, U.S.A.) at 37^{o}C for 2 hr. 3 x 100 µl aliquots were plated onto 50 µg/ml Kanamycin (Thermo Fisher, Massachusetts, U.S.A.) LB plates and grown overnight at 37^{o}C. The remaining volume was left at room temperature overnight and plated on 50 µg/ml Kanamycin and left to grow at 37^{o}C. The knock-out mutation was confirmed using Illumina sequencing.

11. THP-1 macrophage invasion and replication assay

THP-1 monocytes (European Collection of Authenticated Cell Cultures, cat no. 88081201) were plated at $1x10^5$ cells/well in RPMI (Gibco) with 2 mM L-glutamine (Sigma) and 10% fetal bovine serum (Sigma) with PMA (Phorbol 12-myristate 13-acetate, (Sigma) to differentiate to macrophages. After 72 hours, media was changed to the supplemented RPMI (as defined above) for 24h before infection. Bacterial isolates SL1344, D23580, 2101, 9266/3, 12299/3, 6948/3, 9412/3, 10055/3, 8866/3,

12155/3, 10393/3, and 10433/3 were inoculated in 10 mL low-salt lysogeny broth (LB) from frozen stocks and incubated at 37°C, shaking for ~17.5 h prior to use. For infection, bacteria were diluted in PBS to an optical density (OD) of 1 before adding to RPMI. 500 µL of bacteria in media were added to cells for a multiplicity of infection of 20:1 and incubated at 37°C for 30 min. At 30 min, media containing bacteria was removed and replaced with media containing 0.1 mg/ mL gentamicin. For the 1 h invasion timepoint, at 1 h post-infection, cells were washed 1x in PBS then lysed in 1% Triton, and serial dilutions at 10^{-1}, 10^{-2}, 10^{-3} prepared in PBS. 50 µL of each dilution was spotted on LB agar plates in 10 µL spots and incubated at 37°C. For the 6 h intracellular replication timepoint, gentamicin-containing media was replaced by the supplemented RPMI at 1 h post-infection and incubated at 37°C for another 5 h. At 6 h post-infection, cells were washed 1 x in PBS and lysed with 1% Triton, as for the cells at the 1 h timepoint. Agar plates were incubated until colony forming units were visible for counting to calculate viable bacteria per mL. Experiments were done in three biological replicates and mean and standard error of the mean was calculated for all strains.

12. Mouse infection

Salmonella strains were grown static overnight in L broth at 37°C. Inoculations were prepared by diluting overnight culture in PBS. Inoculums were plated post infection on LB agar plates for confirmation. Groups of C57/Bl6 mice were infected intravenously with 2 x 10^2 colony forming units (CFU) or orally with 2 x 10^6 CFU with each *Salmonella* strain. At day 4 post infection mice were culled and organs removed. Homogenised organs were serially diluted in PBS and 20 µl of each dilution

were spotted into LB agar plates. CFUs were counted next day to calculate number of CFUs per organ. All experiments on animals were performed under a UK animal licence that has been through local ethical review before being approved by Sanger - Animal Welfare and Ethical Review Body (AWERB) and performed according to the regulations of the UK Home Office Scientific Procedures Act (1986).

Data and material availability

Sequence data that support the findings of this study have been deposited in SRA with accession codes as listed in Supplementary Table 1. The annotated Pacbio'd reference genome of *Salmonella* Typhimurium strain 10433_3 is uploaded to Genbank with accession ID ERS1310131. The generated phylogenetic tree (as presented in Fig. 2a) is publicly accessible in MicroReact: https://microreact.org/project/ZfwCFTj2-/d9f0ce6f. All other datasets generated during and/or analysed the current study are available from the corresponding author on reasonable request. Requests for obtaining biological material (mutant strains) should be addressed to the corresponding author. Exchange of clinical isolates should always be in agreement with the Institute of Tropical Medicine (Antwerp, Belgium) and Institut National Recherche Biomedicale (Kinshasa, DRC), co-owning the bacterial isolates.

References

1 Crump, J. A., Sjolund-Karlsson, M., Gordon, M. A. & Parry, C. M. Epidemiology, Clinical Presentation, Laboratory Diagnosis, Antimicrobial Resistance, and Antimicrobial Management of Invasive Salmonella Infections. *Clin Microbiol Rev* **28**, 901-937, doi:10.1128/CMR.00002-15 (2015).

2 Reddy, E. A., Shaw, A. V. & Crump, J. A. Community-acquired bloodstream infections in Africa: a systematic review and meta-analysis. *Lancet Infect Dis* **10**, 417-432, doi:10.1016/S1473-3099(10)70072-4 (2010).

3 Keestra-Gounder, A. M., Tsolis, R. M. & Baumler, A. J. Now you see me, now you don't: the interaction of Salmonella with innate immune receptors. *Nat Rev Microbiol* **13**, 206-216, doi:10.1038/nrmicro3428 (2015).

4 Ao, T. T. *et al.* Global burden of invasive nontyphoidal Salmonella disease, 2010(1). *Emerg Infect Dis* **21**, doi:10.3201/eid2106.140999 (2015).

5 Feasey, N. A., Dougan, G., Kingsley, R. A., Heyderman, R. S. & Gordon, M. A. Invasive non-typhoidal salmonella disease: an emerging and neglected tropical disease in Africa. *Lancet* **379**, 2489-2499, doi:10.1016/S0140-6736(11)61752-2 (2012).

6 Kariuki, S. *et al.* Lack of clonal relationship between non-typhi Salmonella strain types from humans and those isolated from animals living in close contact. *FEMS Immunol Med Microbiol* **33**, 165-171, doi:10.1111/j.1574-695X.2002.tb00587.x (2002).

7 Kariuki, S. *et al.* Characterisation of community acquired non-typhoidal Salmonella from bacteraemia and diarrhoeal infections in children admitted to hospital in Nairobi, Kenya. *BMC Microbiol* **6**, 101, doi:10.1186/1471-2180-6-101 (2006).

8 Kariuki, S. *et al.* Invasive multidrug-resistant non-typhoidal Salmonella infections in Africa: zoonotic or anthroponotic transmission? *J Med Microbiol* **55**, 585-591, doi:10.1099/jmm.0.46375-0 (2006).

9 MacLennan, C. A. *et al.* Dysregulated humoral immunity to nontyphoidal Salmonella in HIV-infected African adults. *Science* **328**, 508-512, doi:10.1126/science.1180346 (2010).

10 Branchu, P., Bawn, M. & Kingsley, R. A. Genome Variation and Molecular Epidemiology of Salmonella enterica Serovar Typhimurium Pathovariants. *Infect Immun* **86**, doi:10.1128/IAI.00079-18 (2018).

11 Okoro, C. K. *et al.* Intracontinental spread of human invasive Salmonella Typhimurium pathovariants in sub-Saharan Africa. *Nat Genet* **44**, 1215-1221, doi:10.1038/ng.2423 (2012).

12 Kingsley, R. A. *et al.* Epidemic multiple drug resistant Salmonella Typhimurium causing invasive disease in sub-Saharan Africa have a distinct genotype. *Genome Res* **19**, 2279-2287, doi:10.1101/gr.091017.109 (2009).

13 Kariuki, S. *et al.* Ceftriaxone-resistant Salmonella enterica serotype typhimurium sequence type 313 from Kenyan patients is associated with the blaCTX-M-15 gene on a novel IncHI2 plasmid. *Antimicrob Agents Chemother* **59**, 3133-3139, doi:10.1128/AAC.00078-15 (2015).

14 Feasey, N. A. *et al.* Drug resistance in Salmonella enterica ser. Typhimurium bloodstream infection, Malawi. *Emerg Infect Dis* **20**, 1957-1959, doi:10.3201/eid2011.141175 (2014).

15 Msefula, C. L. *et al.* Genotypic homogeneity of multidrug resistant S. Typhimurium infecting distinct adult and childhood susceptibility groups in Blantyre, Malawi. *PLoS One* **7**, e42085, doi:10.1371/journal.pone.0042085 (2012).

16 Crump, J. A. & Heyderman, R. S. A Perspective on Invasive Salmonella Disease in Africa. *Clin Infect Dis* **61 Suppl 4**, S235-240, doi:10.1093/cid/civ709 (2015).

17 Kalonji, L. M. *et al.* Invasive Salmonella Infections at Multiple Surveillance Sites in the Democratic Republic of the Congo, 2011-2014. *Clin Infect Dis* **61 Suppl 4**, S346-353, doi:10.1093/cid/civ713 (2015).
18 WHO. Background document: The diagnosis, treatment and prevention of typhoid fever. (2003).
19 Langridge, G. C. *et al.* Patterns of genome evolution that have accompanied host adaptation in Salmonella. *Proc Natl Acad Sci U S A* **112**, 863-868, doi:10.1073/pnas.1416707112 (2015).
20 Okoro, C. K. *et al.* Signatures of adaptation in human invasive Salmonella Typhimurium ST313 populations from sub-Saharan Africa. *PLoS Negl Trop Dis* **9**, e0003611, doi:10.1371/journal.pntd.0003611 (2015).
21 Singletary, L. A. *et al.* Loss of Multicellular Behavior in Epidemic African Nontyphoidal Salmonella enterica Serovar Typhimurium ST313 Strain D23580. *MBio* **7**, e02265, doi:10.1128/mBio.02265-15 (2016).
22 Ramachandran, G., Aheto, K., Shirtliff, M. E. & Tennant, S. M. Poor biofilm-forming ability and long-term survival of invasive Salmonella Typhimurium ST313. *Pathog Dis* **74**, doi:10.1093/femspd/ftw049 (2016).
23 Ramachandran, G., Perkins, D. J., Schmidlein, P. J., Tulapurkar, M. E. & Tennant, S. M. Invasive Salmonella Typhimurium ST313 with naturally attenuated flagellin elicits reduced inflammation and replicates within macrophages. *PLoS Negl Trop Dis* **9**, e3394, doi:10.1371/journal.pntd.0003394 (2015).
24 Hammarlof, D. L. *et al.* Role of a single noncoding nucleotide in the evolution of an epidemic African clade of Salmonella. *Proc Natl Acad Sci U S A* **115**, E2614-E2623, doi:10.1073/pnas.1714718115 (2018).
25 Parsons, B. N. *et al.* Invasive non-typhoidal Salmonella typhimurium ST313 are not host-restricted and have an invasive phenotype in experimentally infected chickens. *PLoS Negl Trop Dis* **7**, e2487, doi:10.1371/journal.pntd.0002487 (2013).
26 Lunguya, O. *et al.* Antimicrobial resistance in invasive non-typhoid Salmonella from the Democratic Republic of the Congo: emergence of decreased fluoroquinolone susceptibility and extended-spectrum beta lactamases. *PLoS Negl Trop Dis* **7**, e2103, doi:10.1371/journal.pntd.0002103 (2013).
27 Ley, B. *et al.* Invasive Salmonella enterica serotype typhimurium infections, Democratic Republic of the Congo, 2007-2011. *Emerg Infect Dis* **20**, 701-704, doi:10.3201/eid2004.131488 (2014).
28 Kariuki, S. & Onsare, R. S. Epidemiology and Genomics of Invasive Nontyphoidal Salmonella Infections in Kenya. *Clin Infect Dis* **61 Suppl 4**, S317-324, doi:10.1093/cid/civ711 (2015).
29 Leekitcharoenphon, P. *et al.* Genomics of an emerging clone of Salmonella serovar Typhimurium ST313 from Nigeria and the Democratic Republic of Congo. *J Infect Dev Ctries* **7**, 696-706, doi:10.3855/jidc.3328 (2013).
30 Gomes, C. *et al.* Macrolide resistance mechanisms in Enterobacteriaceae: Focus on azithromycin. *Crit Rev Microbiol* **43**, 1-30, doi:10.3109/1040841X.2015.1136261 (2017).
31 Lubelski, J., Konings, W. N. & Driessen, A. J. Distribution and physiology of ABC-type transporters contributing to multidrug resistance in bacteria.

Microbiol Mol Biol Rev **71**, 463-476, doi:10.1128/MMBR.00001-07 (2007).

32 Thoma, L. & Muth, G. Conjugative DNA transfer in Streptomyces by TraB: is one protein enough? *FEMS Microbiol Lett* **337**, 81-88, doi:10.1111/1574-6968.12031 (2012).

33 Gilmour, M. W., Thomson, N. R., Sanders, M., Parkhill, J. & Taylor, D. E. The complete nucleotide sequence of the resistance plasmid R478: defining the backbone components of incompatibility group H conjugative plasmids through comparative genomics. *Plasmid* **52**, 182-202, doi:10.1016/j.plasmid.2004.06.006 (2004).

34 Prieto, A. I. *et al.* Roles of the outer membrane protein AsmA of Salmonella enterica in the control of marRAB expression and invasion of epithelial cells. *J Bacteriol* **191**, 3615-3622, doi:10.1128/JB.01592-08 (2009).

35 Rivera-Chavez, F. *et al.* Salmonella uses energy taxis to benefit from intestinal inflammation. *PLoS Pathog* **9**, e1003267, doi:10.1371/journal.ppat.1003267 (2013).

36 Wheeler, N. E., Gardner, P. P. & Barquist, L. Machine learning identifies signatures of host adaptation in the bacterial pathogen Salmonella enterica. *PLoS Genet* **14**, e1007333, doi:10.1371/journal.pgen.1007333 (2018).

37 Nuccio, S. P. & Baumler, A. J. Comparative analysis of Salmonella genomes identifies a metabolic network for escalating growth in the inflamed gut. *MBio* **5**, e00929-00914, doi:10.1128/mBio.00929-14 (2014).

38 Tacconelli, E. *et al.* Discovery, research, and development of new antibiotics: the WHO priority list of antibiotic-resistant bacteria and tuberculosis. *Lancet Infect Dis* **18**, 318-327, doi:10.1016/S1473-3099(17)30753-3 (2018).

39 Klemm, E. J. *et al.* Emergence of an Extensively Drug-Resistant Salmonella enterica Serovar Typhi Clone Harboring a Promiscuous Plasmid Encoding Resistance to Fluoroquinolones and Third-Generation Cephalosporins. *MBio* **9**, doi:10.1128/mBio.00105-18 (2018).

40 Magiorakos, A. P. *et al.* Multidrug-resistant, extensively drug-resistant and pandrug-resistant bacteria: an international expert proposal for interim standard definitions for acquired resistance. *Clin Microbiol Infect* **18**, 268-281, doi:10.1111/j.1469-0691.2011.03570.x (2012).

41 Phoba, M. F. *et al.* Multidrug-resistant Salmonella enterica, Democratic Republic of the Congo. *Emerg Infect Dis* **18**, 1692-1694, doi:10.3201/eid1810.120525 (2012).

42 Phoba, M. F. *et al.* Salmonella enterica serovar Typhi Producing CTX-M-15 Extended Spectrum beta-Lactamase in the Democratic Republic of the Congo. *Clin Infect Dis* **65**, 1229-1231, doi:10.1093/cid/cix342 (2017).

43 Falay, D. *et al.* Microbiological, clinical and molecular findings of non-typhoidal Salmonella bloodstream infections associated with malaria, Oriental Province, Democratic Republic of the Congo. *BMC Infect Dis* **16**, 271, doi:10.1186/s12879-016-1604-1 (2016).

44 Agency, E. M. Fluoroquinolon and quinolone antibiotics: PRAC recommends restrictions on use. *European Medicines Agency* (2018).

45 Malhotra-Kumar, S. & Goossens, H. Mass azithromycin distribution and emerging resistance: taking a minimum harms approach. *Clin Infect Dis* **56**, 1527-1529, doi:10.1093/cid/cit139 (2013).
46 Keenan, J. D. *et al.* Azithromycin to Reduce Childhood Mortality in Sub-Saharan Africa. *N Engl J Med* **378**, 1583-1592, doi:10.1056/NEJMoa1715474 (2018).
47 ConfédérationSuisse. Focus RD Congo: Le système sanitaire à Kinshasa : médicaments et soins du VIH-sida, de l'hypertension artérielle, du diabète de type II et des troubles mentaux. (2014).
48 Harrois, D. *et al.* Prevalence and characterization of extended-spectrum beta-lactamase-producing clinical Salmonella enterica isolates in Dakar, Senegal, from 1999 to 2009. *Clin Microbiol Infect* **20**, O109-116, doi:10.1111/1469-0691.12339 (2014).
49 Holt, K. E. *et al.* High-throughput sequencing provides insights into genome variation and evolution in Salmonella Typhi. *Nat Genet* **40**, 987-993, doi:10.1038/ng.195 (2008).
50 McClelland, M. *et al.* Comparison of genome degradation in Paratyphi A and Typhi, human-restricted serovars of Salmonella enterica that cause typhoid. *Nat Genet* **36**, 1268-1274, doi:10.1038/ng1470 (2004).
51 McQuiston, J. R., Fields, P. I., Tauxe, R. V. & Logsdon, J. M., Jr. Do Salmonella carry spare tyres? *Trends Microbiol* **16**, 142-148, doi:10.1016/j.tim.2008.01.009 (2008).
52 Ikeda, J. S. *et al.* Flagellar phase variation of Salmonella enterica serovar Typhimurium contributes to virulence in the murine typhoid infection model but does not influence Salmonella-induced enteropathogenesis. *Infect Immun* **69**, 3021-3030, doi:10.1128/IAI.69.5.3021-3030.2001 (2001).
53 Petrovska, L. *et al.* Microevolution of Monophasic Salmonella Typhimurium during Epidemic, United Kingdom, 2005-2010. *Emerg Infect Dis* **22**, 617-624, doi:10.3201/eid2204.150531 (2016).
54 Mather, A. E. *et al.* New Variant of Multidrug-Resistant Salmonella enterica Serovar Typhimurium Associated with Invasive Disease in Immunocompromised Patients in Vietnam. *MBio* **9**, doi:10.1128/mBio.01056-18 (2018).
55 Grimont, P. A. D. & Weill, F.-X. Antigenic formulae of the *Salmonellae* serovars. *World Health Organization* (2007).
56 CLSI. M100-S28: Performance Standards for Antimicrobial Susceptibility Testing. (2018).
57 Bolger, A. M., Lohse, M. & Usadel, B. Trimmomatic: a flexible trimmer for Illumina sequence data. *Bioinformatics* **30**, 2114-2120, doi:10.1093/bioinformatics/btu170 (2014).
58 Hunt, M. *et al.* Circlator: automated circularization of genome assemblies using long sequencing reads. *Genome Biol* **16**, 294, doi:10.1186/s13059-015-0849-0 (2015).
59 Chin, C. S. *et al.* Nonhybrid, finished microbial genome assemblies from long-read SMRT sequencing data. *Nat Methods* **10**, 563-569, doi:10.1038/nmeth.2474 (2013).
60 Seemann, T. Prokka: rapid prokaryotic genome annotation. *Bioinformatics* **30**, 2068-2069, doi:10.1093/bioinformatics/btu153 (2014).

61 Pruitt, K. D., Tatusova, T., Brown, G. R. & Maglott, D. R. NCBI Reference Sequences (RefSeq): current status, new features and genome annotation policy. *Nucleic Acids Res* **40**, D130-135, doi:10.1093/nar/gkr1079 (2012).
62 Li, H. *et al.* The Sequence Alignment/Map format and SAMtools. *Bioinformatics* **25**, 2078-2079, doi:10.1093/bioinformatics/btp352 (2009).
63 Croucher, N. J. *et al.* Rapid phylogenetic analysis of large samples of recombinant bacterial whole genome sequences using Gubbins. *Nucleic Acids Res* **43**, e15, doi:10.1093/nar/gku1196 (2015).
64 Page, A. J. *et al.* SNP-sites: rapid efficient extraction of SNPs from multi-FASTA alignments. *Microb Genom* **2**, e000056, doi:10.1099/mgen.0.000056 (2016).
65 Stamatakis, A. RAxML version 8: a tool for phylogenetic analysis and post-analysis of large phylogenies. *Bioinformatics* **30**, 1312-1313, doi:10.1093/bioinformatics/btu033 (2014).
66 Letunic, I. & Bork, P. Interactive tree of life (iTOL) v3: an online tool for the display and annotation of phylogenetic and other trees. *Nucleic Acids Res* **44**, W242-245, doi:10.1093/nar/gkw290 (2016).
67 Argimon, S. *et al.* Microreact: visualizing and sharing data for genomic epidemiology and phylogeography. *Microb Genom* **2**, e000093, doi:10.1099/mgen.0.000093 (2016).
68 Bouckaert, R. *et al.* BEAST 2: a software platform for Bayesian evolutionary analysis. *PLoS Comput Biol* **10**, e1003537, doi:10.1371/journal.pcbi.1003537 (2014).
69 Drummond, A. J., Ho, S. Y., Phillips, M. J. & Rambaut, A. Relaxed phylogenetics and dating with confidence. *PLoS Biol* **4**, e88, doi:10.1371/journal.pbio.0040088 (2006).
70 Heled, J. & Drummond, A. J. Bayesian inference of population size history from multiple loci. *BMC Evol Biol* **8**, 289, doi:10.1186/1471-2148-8-289 (2008).
71 Wheeler, N. E., Barquist, L., Kingsley, R. A. & Gardner, P. P. A profile-based method for identifying functional divergence of orthologous genes in bacterial genomes. *Bioinformatics* **32**, 3566-3574, doi:10.1093/bioinformatics/btw518 (2016).
72 Li, H. & Durbin, R. Fast and accurate short read alignment with Burrows-Wheeler transform. *Bioinformatics* **25**, 1754-1760, doi:10.1093/bioinformatics/btp324 (2009).
73 Li, H. A statistical framework for SNP calling, mutation discovery, association mapping and population genetical parameter estimation from sequencing data. *Bioinformatics* **27**, 2987-2993, doi:10.1093/bioinformatics/btr509 (2011).
74 Hunt, M. *et al.* ARIBA: rapid antimicrobial resistance genotyping directly from sequencing reads. *Microb Genom* **3**, e000131, doi:10.1099/mgen.0.000131 (2017).
75 McArthur, A. G. *et al.* The comprehensive antibiotic resistance database. *Antimicrob Agents Chemother* **57**, 3348-3357, doi:10.1128/AAC.00419-13 (2013).

76 Inouye, M. *et al.* SRST2: Rapid genomic surveillance for public health and hospital microbiology labs. *Genome Med* **6**, 90, doi:10.1186/s13073-014-0090-6 (2014).
77 Alikhan, N. F., Petty, N. K., Ben Zakour, N. L. & Beatson, S. A. BLAST Ring Image Generator (BRIG): simple prokaryote genome comparisons. *BMC Genomics* **12**, 402, doi:10.1186/1471-2164-12-402 (2011).
78 Page, A. J. *et al.* Robust high-throughput prokaryote de novo assembly and improvement pipeline for Illumina data. *Microb Genom* **2**, e000083, doi:10.1099/mgen.0.000083 (2016).
79 Darling, A. C., Mau, B., Blattner, F. R. & Perna, N. T. Mauve: multiple alignment of conserved genomic sequence with rearrangements. *Genome Res* **14**, 1394-1403, doi:10.1101/gr.2289704 (2004).
80 Romling, U. Characterization of the rdar morphotype, a multicellular behaviour in Enterobacteriaceae. *Cell Mol Life Sci* **62**, 1234-1246, doi:10.1007/s00018-005-4557-x (2005).
81 Kritikos, G. *et al.* A tool named Iris for versatile high-throughput phenotyping in microorganisms. *Nat Microbiol* **2**, 17014, doi:10.1038/nmicrobiol.2017.14 (2017).
82 R_Core_Team. R: A language and environment for statistical computing. *R Foundation for Statistical Computing, Vienna, Austria.* **URL https://www.R-project.org/.** (2017).
83 Vaas, L. A. *et al.* opm: an R package for analysing OmniLog(R) phenotype microarray data. *Bioinformatics* **29**, 1823-1824, doi:10.1093/bioinformatics/btt291 (2013).
84 Hothorn, T., Bretz, F. & Westfall, P. Simultaneous inference in general parametric models. *Biom J* **50**, 346-363, doi:10.1002/bimj.200810425 (2008).
85 Datsenko, K. A. & Wanner, B. L. One-step inactivation of chromosomal genes in Escherichia coli K-12 using PCR products. *Proc Natl Acad Sci U S A* **97**, 6640-6645, doi:10.1073/pnas.120163297 (2000).

Acknowledgements

We are grateful to Ado Van Assche (K.U. Leuven, Leuven, Belgium), Eke van Zwol and Janah Vandenhoeck (Institute of Tropical Medicine, ITM, Antwerp, Belgium) for assistance with Biolog experiments; to Simon Harris, Jacqueline Keane, Nick Thomson and the Pathogen Informatics team (Wellcome Sanger Institute, Hinxton, Cambridge, United Kingdom) for the support and Bieke Tack for critical reading. This work was funded by the Belgian Directorate of Development Cooperation (DGD) through Project 2.01 of the Third Framework Agreement between the Belgian DGD and ITM, Belgium; the Flemish Interuniversity Council (VLIR-UOS); the

Flemish Ministry of Sciences (EWI; SOFI project IDIS and fellowship S.V.P); the Baillet Latour Fund (The Bacterial Infections in the Tropics (BIT) research cluster at ITM Antwerp, Belgium); the FWO Research Foundation – Flanders (travel grant to S.V.P.) and the Wellcome Trust. GD is supported by The Wellcome Trust and the NIMR BRC AMR Theme at Cambridge.

Author contributions

Study design and oversight: SVP, JJ, GD, SD

Data analysis: SVP, KV, EH, NW, EJK

Isolate acquisition and processing and clinical data collection: JJ, BB, LK, LMK, M-FP, DF, DN, OL

Wet lab and infection experiments: DP, TdB, SC, EC, KH, SS, EL

Manuscript writing: SVP, JJ, GD, SD

All authors contributed to manuscript editing.

Competing Interests statement

The authors declare no competing interests.

Figure Legends

Figure 1: Geographical origin of *S.* Typhimurium showing extended spectrum beta-lactamase (ESBL) production and azithromycin (AZI) resistance in the Democratic Republic of the Congo.

Red dots with numbers (n) of the included resistant strains in the respective surveillance sites (Kinshasa, Kisangani and Kisantu).

Figure 2: The population structure of *S.* Typhimurium ST313 in Africa and the emergence of a new sublineage ST313 II.1

a. Maximum likelihood phylogenetic tree based on the 81 genome sequences from this study and 153 African and 42 non-African publicly available *S.* Typhimurium strains (summarized in Supplemental Table 2). Sequencing reads were mapped against *S.* Typhimurium ST313 lineage II reference strain D23580 [12]. The tree is based on 62884 chromosomal SNPs. Branches of *S.* Typhimurium ST313 sublineage II.1 are colored in red. Metadata is visualized on the concentric rings in compliance to the legend, from the inside to outside; 1. Country of origin, 2. Year of isolation, 3. Presence of IncHI2 replicon, 4-8. Presence of multidrug resistance markers (MDR; *bla, cat, sul, dfrA*), *mphA, blaSHV-2A, qnrS* and *gyrA* antimicrobial resistance markers (AMR). Reference strains A130 (lineage I), D23580 (lineage II) and 10433_3 (sublineage II.1) are indicated in blue, as well as strain 5390_4. Branch lengths represent the number of SNPs as indicated in the scale bar. The tree is publicly available on microreact (https://microreact.org/project/ZfwCFTj2-/d9f0ce6f; Supplemental Fig. 2).

b. Maximum likelihood phylogenetic tree of all *S.* Typhimurium ST313 lineage II strains included in this study, based on mapping against sublineage II.1 reference strain 10433_3 (this study). The tree is based on 1207 chromosomal SNPs. A collapsed branch is annotated with a grey triangle. The tree is rooted with *S.* Typhimurium strain DT2B, a European ST313 strain. Branches of *S.* Typhimurium ST313 sublineage II.1 are colored in red. Metadata is visualized lanes in compliance to the legend, from left to right; 1. Country of origin, 2.

Year of isolation, 3. Presence of IncHI2 replicon, 4-8. Presence of multidrug resistance markers (MDR; *bla, cat, sul, dfrA*), *mphA, blaSHV-2A, qnrS* and *gyrA* AMR markers. 9. Location in the Democratic Republic of the Congo. Reference strain 10433_3 (sublineage II.1) is indicated in blue. Branch lengths are indicated and represent the number of SNPs.

Figure 3: Bayesian time-tree of African *S.* Typhimurium ST313 lineage II

Bayesian maximum clade credibility phylogeny of African *S.* Typhimurium ST313 lineage II and sublineage II.1 isolates. The time-tree is based on 1187 SNP differences detected across the whole core genome of the 175 lineage II and II.1 sequenced isolates. The tree was visualized and colored in Figtree v1.4.2. A divergence date (median estimate and its respective 95% HPD) is indicated for the ST313 II.1 sublineage. Tree tips are color coded according to their country of origin (colored by legend at top).

Figure 4: IncHI2 resistance plasmid pCST313 from *S.* Typhimurium ST313 sublineage II.1

The genetic makeup of the pCST313 resistance plasmid from isolate 10433_3 is given. pCST313 is 274,695 nucleotides long, and has 290 annotated genes. Annotations are shown on the outer circle and coloured by gene function: resistance genes (red), plasmid functions (blue), transposon related genes (green), metabolism functions (white) and hypothetical genes (grey). The inner five circles show pairwise similarity regions of 100 % with previously reported IncHI2 plasmids in *S.* Typhimurium ST313 (pKST313 from Kenya (LN794248) and pSTm-A54650 from Malawi (LK056646)), a draft assembly from the IncHI2 plasmid of strain 5390_4

from Kisangani (this study) and R478 IncHI2 from *Serratia marescens* isolated in the USA (BX664015).

Figure 5: Genomic changes in *S.* Typhimurium ST313 sublineage II.1 versus ST313 lineage II

An schematic overview of the genomic differences between *S.* Typhimurium ST313 sublineage II.1 versus ST313 lineage II are schematically shown. The genetic changes in *S.* Typhimurium sublineage II.1 include the acquisition of a new resistance plasmid, pCST313, the loss of the flagellin *fljB* gene and the acquisition of 38 single nucleotide polymorphisms (SNPs) in the chromosome sequence.

Figure 6: Increased host adaptation of sublineage II.1

a. Invasiveness index values for all *S.* Typhimurium sequences included in this study, grouped into lineage, as calculated by the method of Wheeler et al. (2018). Summary of statistics on different clades: Non-ST313: median = 0.184, SD = 0.093; Lineage I: median = 0.185, SD = 0.003; Lineage II: median = 0.205, SD = 0.005; Lineage II.1: median = 0.222, SD = 0.004. The groups were compared using a Mann Whitney U test. Boxplot center lines represent median values, box limits present upper and lower quartiles; whiskers the 1.5 interquartile range and points the outliers.

b. Red, dry and rough (RDAR) morphotype [80] of *S.* Typhimurium ST313 lineage II strain D23580 [12], *S.* Typhimurium ST313 lineage II.1 strain 10433_3 (this study) and a *S.* Typhimurium ST313 lineage II D23580 *asmA* knock-out strain (this study).

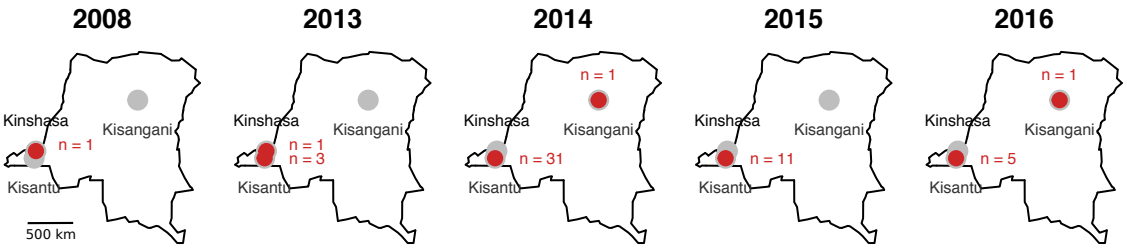
2008
Kinshasa
Kisangani
n = 1
Kisantu
500 km
2013
Kinshasa
Kisangani
n = 1
n = 3
Kisantu
2014
n = 1
Kinshasa
Kisangani
n = 31
Kisantu
2015
Kinshasa
Kisangani
n = 11
Kisantu
2016
n = 1
Kinshasa
Kisangani
n = 5
Kisantu

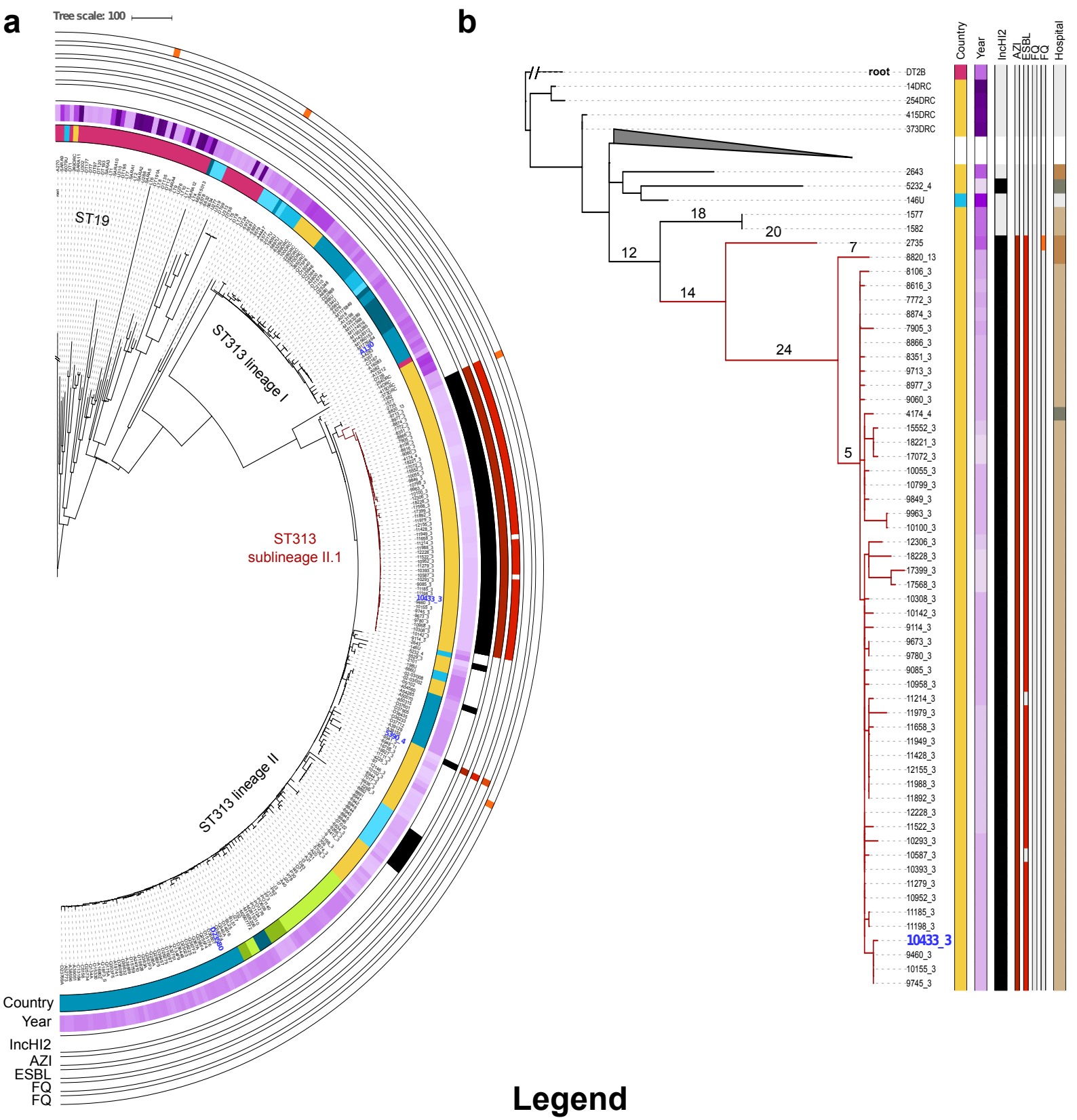

Legend

Country

- Mali
- Nigeria
- D.R. Congo
- Kenya
- Uganda
- Malawi
- Mozambique
- Non-African

Year

1938

2016

AMR genetic markers

- IncHI2 plasmid
- *mphA* (AZI)
- *blaSHV-2A* (ESBL)
- *qnrS* (FQ)
- *gyrA* (FQ)

Hospital

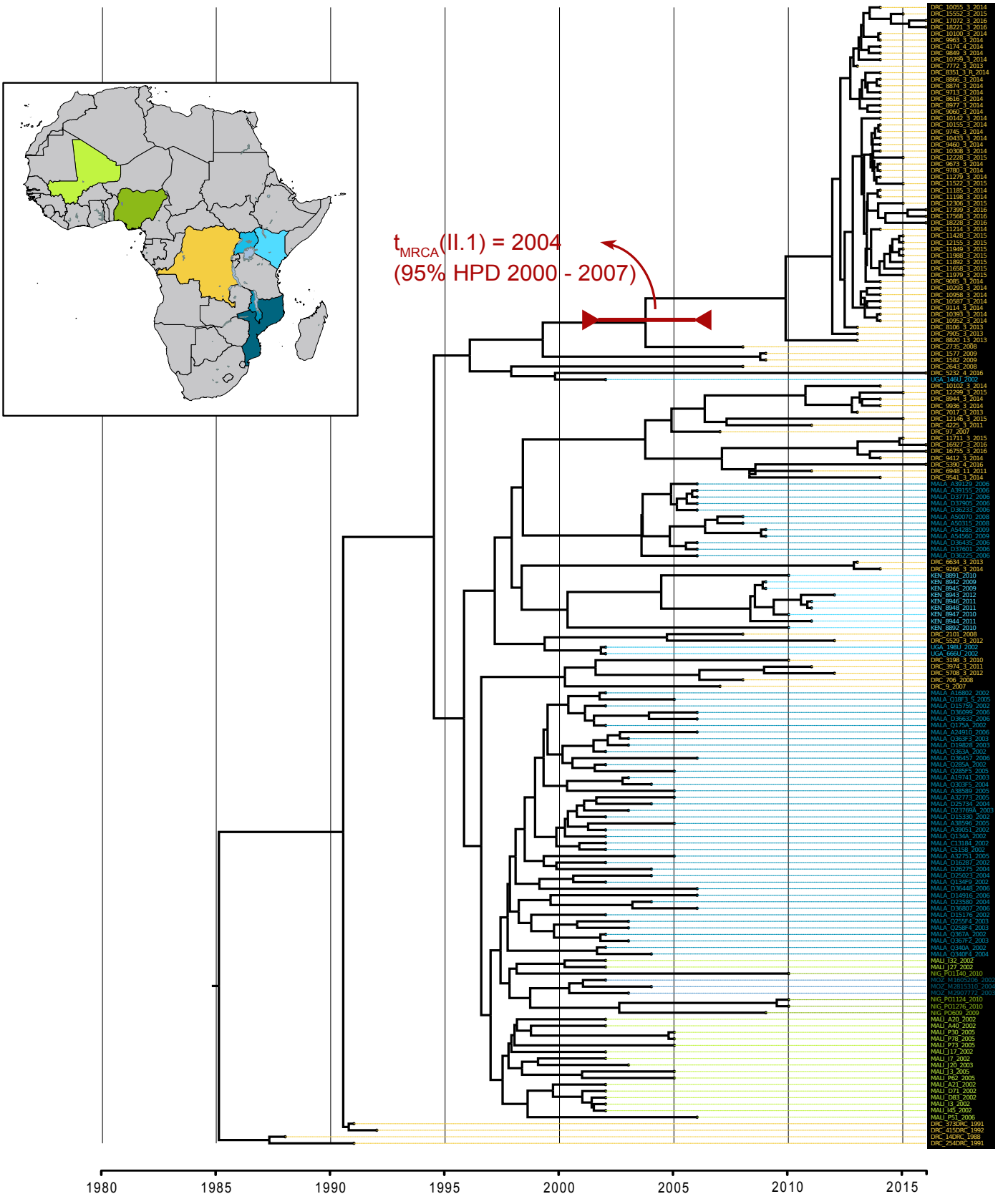
t_{MRCA}(II.1) = 2004
(95% HPD 2000 - 2007)
1980
1985
1990
1995
2000
2005
2010
2015

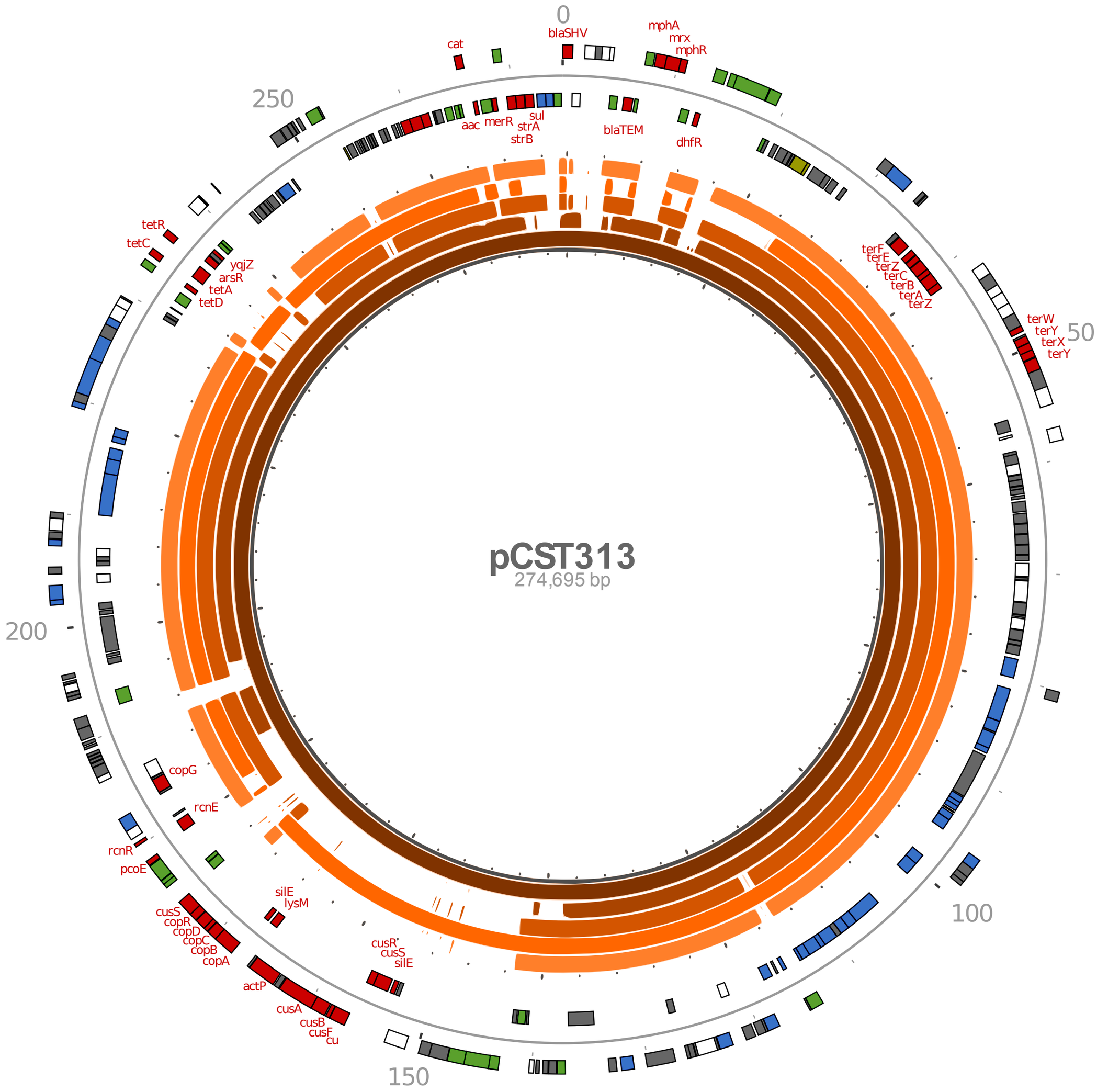

Annotation

- Resistance
- Transposon
- Plasmid functions
- Metabolism
- Hypothetical

Pairwise similarity

- pCST313
- p5390_4
- pKST313
- R478
- pSTM-A54650

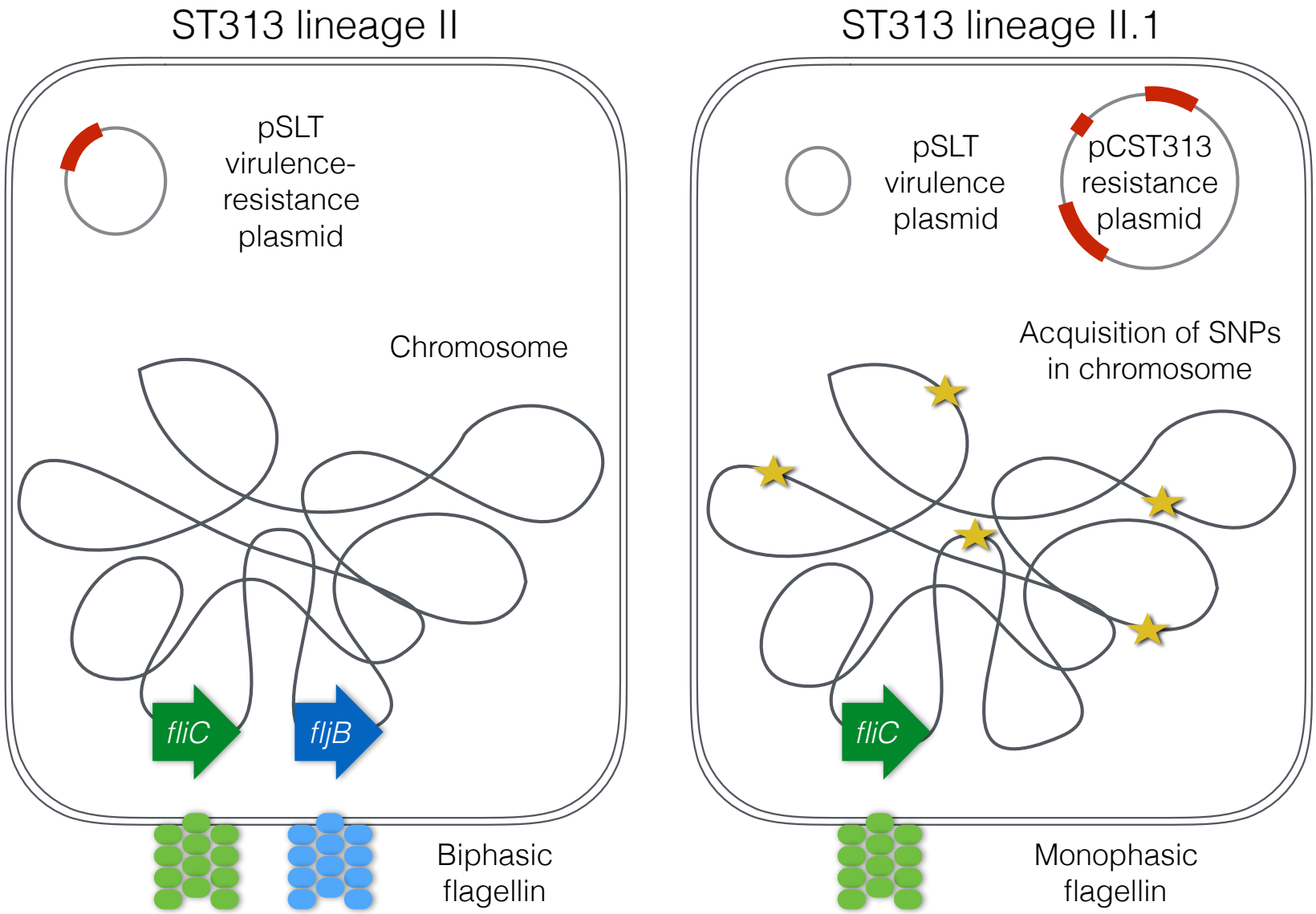
ST313 lineage II
pSLT
virulence-
resistance
plasmid
Chromosome
fliC
fljB
Biphasic
flagellin
ST313 lineage II.1
pSLT
virulence
plasmid
pCST313
resistance
plasmid
Acquisition of SNPs
in chromosome
fliC
Monophasic
flagellin

a

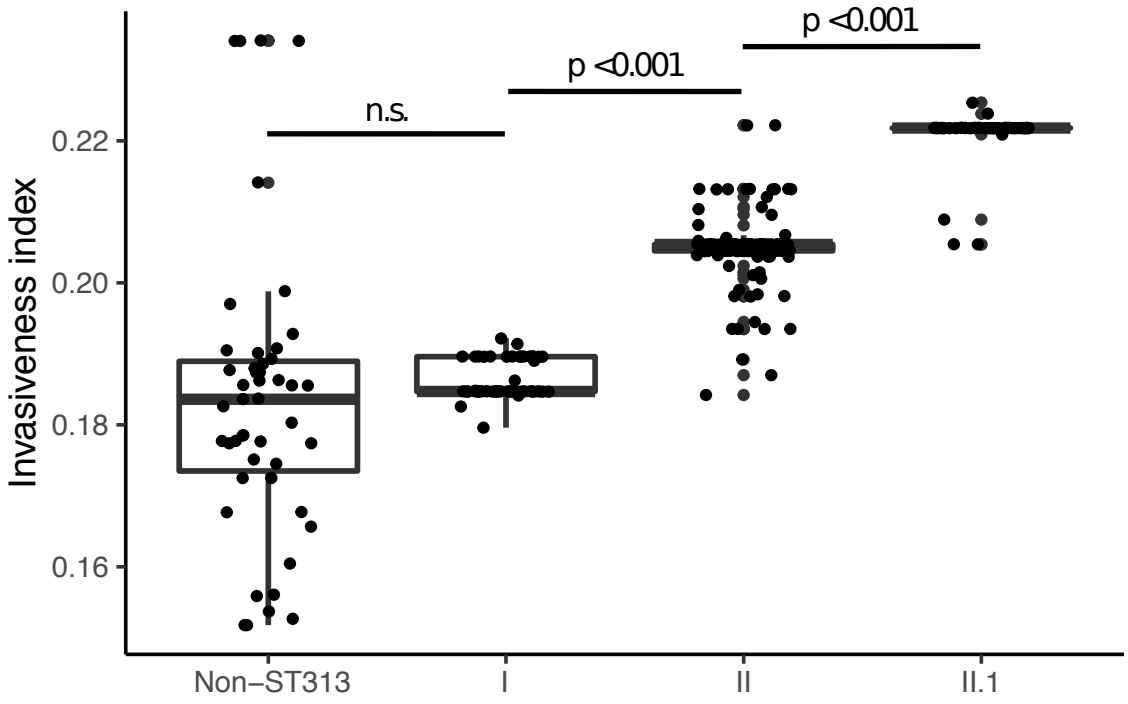
p <0.001
p <0.001
n.s.
Invasiveness index
0.22
0.20
0.18
0.16
Non−ST313
I
II
II.1

b

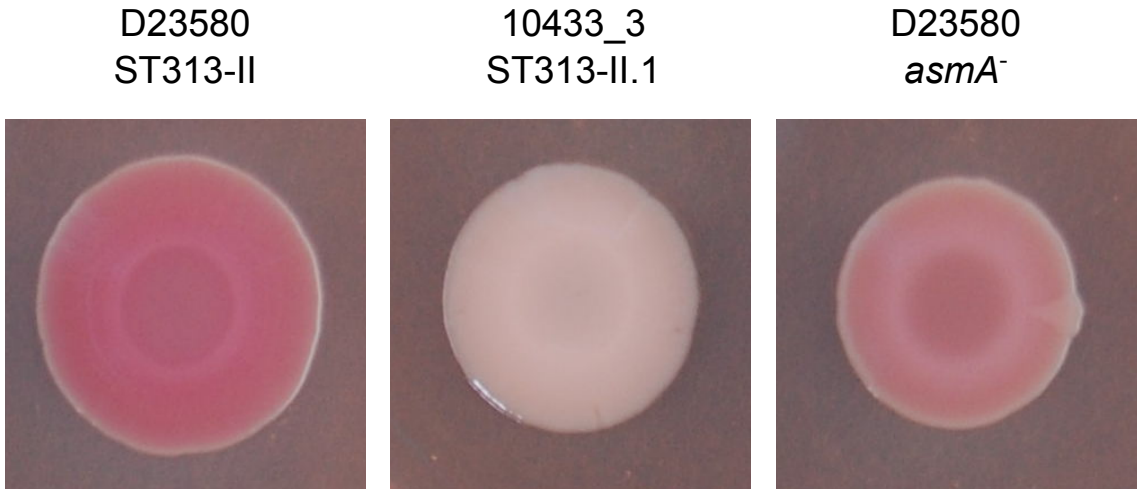
D23580
ST313-II
10433_3
ST313-II.1
D23580
asmA-